Computational Analyses of Docosahexaenoic Acid (DHA, C22:6, n-3) with Alzheimer's Disease-Causing Amyloid Peptide A$\beta_{1\text{-}42}$ Reassures Its Therapeutic Utility

Michio Hashimoto[1*], Shahdat Hossain[1,2], Kentaro Matsuzaki[1], Abdullah Al Mamun[1], Hiroyuki Arai[3], Osamu Shido[1]

[1]Department of Environmental Physiology, Faculty of Medicine, Shimane University, Izumoshi, Japan
[2]Laboratory of Alternative Medicine and Behavioral Neurosciences, Department of Biochemistry and Molecular Biology, Jahangirnagar University, Dhaka, Bangladesh
[3]Department of Geriatrics and Gerontology, Division of Brain Sciences, Institute of Development, Aging and Cancer, Tohoku University, Sendai, Japan
Email: *michio1@med.shimane-u.ac.jp, shahdat@dhaka.net, matuzaki@med.shimane-u.ac.jp, mamun104@gmail.com, harai@idac.tohoku.ac.jp, o-shido@med.shimane-u.ac.jp

Abstract

The accumulation of amyloid *β* peptide$_{1\text{-}42}$ (A$\beta_{1\text{-}42}$) masses in the brains of Alzheimer's Disease (AD) patients is associated with neuronal loss and memory deficits. We have previously reported that oral administration of docosahexaenoic acid (DHA, C22:6, n-3) significantly decreases A*β* burden in the brains of AD model rats and that direct *in vitro* incubation of DHA with A$\beta_{1\text{-}42}$ curbs the progression of amyloid fibrillation. In the present *in silico* study, we investigated whether DHA computationally binds with amyloid peptides. The NMR solution structures of A$\beta_{1\text{-}42}$ were downloaded from the Protein Data Bank (PDB IDs: 1Z0Q and 2BEG). The binding of DHA to A*β* peptides was assessed by molecular docking using both a flexible and rigid docking system. Thioflavin T (ThT) was used as positive control. The chemical structures of ThT and DHA were modeled and converted to the PDB format using PRODRUG. Drug-like properties of DHA were evaluated by ADME (Absorption, Distribution, Metabolism, and Excretion). DHA was found to successfully dock with A$\beta_{1\text{-}42}$. Computational analyses of the binding of DHA to A$\beta_{1\text{-}42}$, as evaluated by docking studies, further corroborated the inhibitory effect of DHA on *in vitro* A$\beta_{1\text{-}42}$ fibrillogenesis and might explain the *in vivo* reduction of amyloid burden observed in the brains of DHA-administered AD model rats demonstrated in our previous study. These computational data suggest the potential utility of DHA as a preventive medication in A*β*-induced neurodegenerative diseases, including AD.

---

*Corresponding author.

Keywords

Docosahexaenoic Acid, Alzheimer's Disease, Amyloid Beta Peptide, Molecular Docking, *In Silico*, Drug Design, Protein Data Bank

1. Introduction

Alzheimer's Disease (AD), a progressive neurodegenerative disease, is the most common cause of dementia in elderly people [1] [2]. Clinically, it is characterized by loss of memory, inability to learn new things, loss of language function, a disturbed perception of space, inability to do calculations, and a host of other manifestations [3]. In AD, there is an overall shrinkage of brain tissue, whereas, it is microscopically characterized by extracellular (neuritic plaques) and/or intracellular (neurofibrillary tangles) deposition of insoluble amyloid beta peptides (Aβs) [4]. Aβ is a peptide with 42 or 43 amino acids that forms a part of the transmembrane domain of the larger Amyloid Precursor Protein (APP), a transmembrane protein expressed in neurons and other brain cells and is derived from the cleavage of APP by the β- and γ-secretase enzymes [5]-[7]. Defective clearance of Aβ from aberrant cleavage of APP and other mechanisms results in its accumulation [8] [9]. Aβ monomers initially polymerize into soluble oligomers and subsequently into larger insoluble fragments which precipitate as amyloid fibrils [10]. The beta amyloid hypothesis suggests that AD is caused by the deposition of Aβ in plaques in brain tissue and is the basis of a novel prevention and treatment method for AD [11]. Indeed, AD animal models can be produced by brain ventricular infusion of Aβ_{1-42} [12] [13]. Moreover, other fragments of Aβs, such as Aβ_{1-40} [14]-[16] and Aβ_{25-35} [17], have also been shown to assemble into amyloid fibers *in vitro* [16] [18] and have been infused into rat brain ventricles to create AD animal models. Because AD has been shown to be associated with decreased Docosahexaenoic Acid (DHA) levels [19] [20], numerous human trials are currently ongoing to determine whether DHA is effective in the treatment and/or delaying the symptoms of AD [21] [22]. We also reported that DHA decreases amyloid burden in the brains of Aβ-infused model rats [14] [15] and inhibits *in vitro* amyloid fibrillation [16] [18]. These investigations highlight the potential for DHA as an excellent therapeutic agent against Aβ-induced neurodegenerative diseases, including AD.

Previously, we showed that DHA inhibits Aβ fibril formation [10] [14]-[16] [18]. In this study, we investigated the computational binding of DHA to Aβ peptides to further support the anti-Aβ fibrillation effect of DHA. Because X-ray crystallographic structures of Aβs are not available, NMR structures were utilized in the present investigation. We performed molecular docking studies, which are useful for identifying agents capable of inhibiting proteins responsible for disease pathology and exploring their possible binding modes. We used thioflavin-T (ThT) as a positive control because it is currently used as a "standard" for selectively binding, staining, and identifying amyloid fibrils both *in vivo* and *in vitro* [23]. We docked DHA and ThT (as ligands) onto Aβ_{1-42} (as receptors) and compared their binding modes. We aimed to confirm the results of our previous studies, showing the ameliorative effects of DHA and its potential as an AD therapy, in this computational analysis [10] [13]-[16] [18].

2. Methods and Materials

2.1. Preparation of Thioflavin T and Docosahexaenoic Acid Models

DHA (CID: 445580) and ThT (CID: 16953) were downloaded from the PubChem database in sdf format. The sdf files were submitted to the PRODRG server [24] to give energy-minimized structures of the ligands. Energy minimization is performed to help the docking program identify the bioactive conformer from the local minima. The two-dimensional structures of ligands are illustrated as ball and stick in **Figure 1**.

2.2. Analyses of Drug-Like Properties of the Ligands

Drug design essentially focuses on optimizing the binding interactions of ligands with their targets. However, a compound with the best binding interactions does not necessarily make the best drug, as other factors are involved. For example, a clinically useful drug must travel through the body to reach its target. Perfecting a compound with good drug-target interactions is irrelevant if it has no chance of reaching its target. The factors that
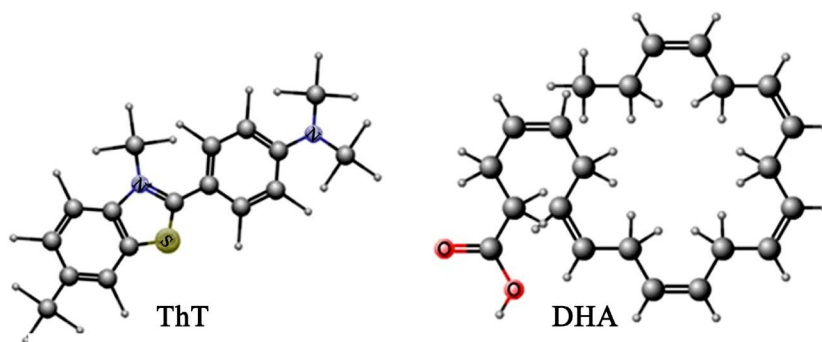
Figure 1. The ligand molecules thioflavin T (ThT) and docosahexaenoic acid (DHA, C22:6, n-3).

determine whether a drug will reach its target in the body are termed the pharmacokinetic or ADME (Absorption, Distribution, Metabolism, and Excretion) properties. We used the free ADME/tox filtering tool (FAF-Drugs 3), which can predict whether the physicochemical properties of compounds are acceptable by applying several filtering rules, including the well-known Lipinski's rule of five (*i.e.*, molecular weight > 500, logP or octanol/water partition coefficient < 5, number of H-bond donors < 5, and number of H-bond acceptors < 10) [Lipinski *et al.*, 2001] [25]. The main properties computed by FAF-Drugs 3 are the number of rigid and flexible bonds, topological polar surface area (TPSA) value according to Ertl *et al.* (2000) [26], number and maximum size of system rings, and presence of unwanted chemicals or chemical substructures (using SMARTS searches) [27].

2.3. Analysis of the Amyloidogenic Regions in the Aβ_{1-42} and Cross-Beta Aggregation

Sequence-based computational methods, namely FoldAmyloid [28], AGGRESCAN [29], and ProA [30], were used to predict the amyloidogenic regions in Aβ_{1-42}. Furthermore, analysis of the beta-aggregation propensity of Aβ_{1-42} was achieved by subjecting the primary amino acid sequence of Aβ_{1-42} to the TANGO algorithm [31]-[33], which is designed to predict cross-beta aggregation in peptides.

2.4. Preparation of Aβ_{1-42} Receptor Models

The three-dimensional solution structures (3D NMR) of Aβ_{1-42} (PDB IDs: 2BEG and 1Z0Q) were downloaded from the RCSB Protein Data Bank (PDB) (http://www.rcsb.org/) as receptors for ThT and DHA docking. 2BEG is a homopentamer, namely composed of the A, B, C, D, and E monomers of Aβ_{1-42}. Each monomer (A, B, C, D, and E) of 2BEG comprises 10 coordinate models [9]. The coordinates of model 1 of the A monomer (A1), model 1 of the B monomer (B1), and model 1 of the C monomer (C1) were loaded in the Molegro virtual docker (MVD) and split from the composite 2BEG PDB file. Accordingly, 1Z0Q is a homo 30-mer composed of 30-monomers (A), each comprising an individual coordinate model. The A1 monomer was split from the composite 1Z0Q PDB file. At least two amyloid molecules are required to achieve the repeating structure of a protofilament fibril. Therefore, the dimer (**Figure 2**) or the trimer (**Figure 6**) models were generated by RossettaDock [34], as described previously [35]. Subsequently, the generated dimers (A1B1) or trimers (A1B1C1) were utilized for ThT and DHA docking (both flexible and rigid docking).

2.5. Computational Analysis of Binding Sites in Aβ_{1-42} Dimers or Trimers

The binding sites or pockets of the dimer (A1B1) and trimer (A1B1C1) were determined by GHECOM, which detects grid-based pockets/binding sites on the surface/interior of the protein [36]. The program produces a graph of residue-based "pocketness," and the presence of binding sites was visualized using the 3D molecular viewer Jmol [37].

2.6. Inter-Surface Interaction Site Analysis of the Aβ_{1-42} Dimer (A1B1)

Protein-protein (the monomer-monomer A1B1 dimer) inter-surface interaction sites were analyzed by feeding the A1B1 dimer to the cons-PPISP server [38], which predicts the residues that are likely to form the binding site for neighboring proteins. The energy distribution along the protein-protein interface is not homogenous;
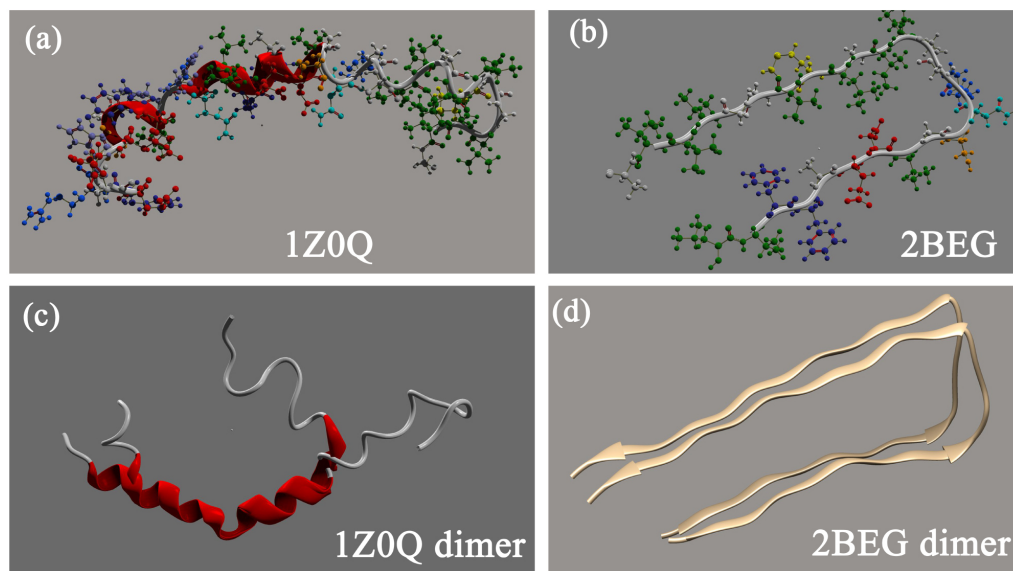
Figure 2. The monomeric structure files for Aβ$_{1\text{-}42}$ were prepared from their parent composite PDB files (2BEG and 1Z0Q). Subsequently, dimers of Aβ$_{1\text{-}42}$ were formed in order to dock ligands (ThT and DHA). (a), (b) Monomer; (c), (d) Dimer.

certain residues contribute more to the binding free energy, called "hot spots." Hot-point servers predict hot spots in protein interfaces using an empirical model that incorporates a few simple rules consisting of occlusion from solvent and total knowledge-based pair potentials of residues [39]. To further validate the presence of inter-surface hotpoints on the dimer interface binding contacts, the dimer was fed to hot-point prediction servers, including Knowledge-based FADE and Contacts (KFC2) [40].

2.7. Molecular Docking Simulations of ThT and DHA onto the Aβ$_{1\text{-}42}$ Dimer

The molecular docking simulations were performed using MVD [41] and PatchDock [42].

2.7.1. Molegro Virtual Docker (MVD)

MVD version 4.3.0 (free academic version), along with its graphical user interface (MVD tools), was utilized to generate a grid, calculate the dock score, and evaluate conformers. The nonpolar hydrogen atoms were removed from the receptor file and their partial charges were added to the corresponding carbon atoms. Docking was performed by following the steps in the MVD user manual [41]. MolDock score of ligands were calculated during docking. MVD performs flexible ligand docking with optimization of the ligand geometry during docking. Therefore, bond angles, bond lengths, and torsional angles of the ligand are modified during the stages of receptor-ligand complex generation.

2.7.2. PatchDock

PatchDock is a shape complementarity/geometry-based molecular docking algorithm. It is aimed at finding docking transformations that yield good molecular shape complementarity. Such transformations induce both wide interface areas and small amounts of steric clashes. A wide interface is ensured to include several matched local features of the docked molecules that have complementary characteristics. The output of PatchDock is a list of candidate complexes between the receptor and ligand molecules. The list is sorted according to geometric shape complementarity score, approximate interface area of the receptor-ligand complex, atomic contact energy (ACE) between ligand and receptor, and 3D transformation. Finally, the server provides an option to download the ligand-receptor complexes in the PDB format. The PatchDocked ligand-receptor complex (of Rank 1) was visualized using PyMOL [43].

3. Results

The predicted physical (ADME) properties of DHA and ThT, as evaluated by the FAF-Drug 3, are shown in

Table 1. The major difference between the properties of DHA and ThT was in the LogP (octanol-water partition coefficient) value, which was >5 for DHA, but <5 for ThT. Thus, DHA violated Lipinski's rule of five and this may relate to the more hydrophobic acyl chains in DHA compared with those in ThT. Partition coefficients indicate the distribution of drugs within the body. Hydrophobic drugs with high octanol/water partition coefficients are mainly distributed to hydrophobic areas such as lipid bilayers of cells. The number of rotatable flexible bonds helps a molecule to adopt 3D structure with a greater flexibility, while that of the rigid bonds performs the opposite trend. Molecular polar surface area (PSA) is a very useful parameter for prediction of drug transport properties. Polar surface area is defined as a sum of surfaces of polar atoms (usually oxygens, nitrogens and attached hydrogens) in a molecule. This parameter is used to correlate very well with the human intestinal absorption, monolayers permeability, and blood-brain barrier penetration. Usually, the molecules with a polar surface area of greater than 120 - 140 Å^2 tend to be poor in permeating cell membranes. The oral bioavailability scores based on solubility in water (Sw) were 2.29×10^{-5} and 2.14×10^{-5} for DHA and ThT, respectively. The log of these two values, *i.e.* Sw, was −4.64 and −4.67, respectively. This indicates that the water solubility of these two compounds were comparable. Because of the Lipinski's rules (LR) are based on physicochemical criteria for physiological effect of drugs (ADME mainly) but does not rule out a possible direct interaction between a molecule and a protein outside the cellular context. Moreover, LRs are violated by numerous drugs or physiologically relevant molecules. Notably, the LR is a group of physicochemical properties used to evaluate the probability of a substance to become an effective drug. However, the conclusions that can be drawn from a docking exercise are limited. If a docking is good and a ligand gets a good score, this just suggests that the compound might have activity against a given target. Docking says nothing about physicochemical properties.

Aggregation-propensity analyses of the Aβ_{1-42} peptides are shown in **Table 2**. The hot-spot analyses by FoldAmyloid [28], AGGRESCAN [29], and ProA [30] revealed that the amino acid residues from Val24 to Lys28/ Gly29 and those from Val39 to Ala42 were the most susceptible to amyloidogenesis.

Beta-aggregation propensity analysis also revealed that the amino acid residues from Lys16 to Asp23, and those from Lys28 to Ala42, displayed the highest beta-aggregation tendency (**Figure 3**). These two regions (Lys16-Asp23 and Lys28-Ala42) may adopt β-sheet secondary structures, and hence, have a higher beta-aggregation propensity during fibrillation.

When a protein molecule binds to another biological polymer (protein) to form a complex, the subset of residues in the interface that account for most of the protein binding free energy are called binding *hot spots*. Therefore,

Table 1. *In silico*-predicted ADME properties of DHA and ThT using FAF-*Drugs* 3 properties.

Properties	DHA	ThT
MW (molecular weight)	330.50	283.41
LogP (octanol-water partition coefficient)	5.84	4.66
LogSw (oral bioavailability scores based on solubility in water)	−4.64	−4.67
tPSA (topological polar surface area, Å^2)	40.46	31.78
Number of rotatable bonds	14	2
Number of rigid bonds	6	16
Flexibility	0.70	0.11
Hydrogen Bond Donor (HBD)	2	0
Hydrogen Bond Acceptor (HBA)	2	2
Number of heavy atoms	24	20
Number of carbon atoms	22	17
Number of heteroatoms	2	3
*Number of lipinski violations	1	0
Solubility	3178.13	2665.28

FAF-*Drugs* 3 evaluated drug-like properties of ThT and DHA. FAF-*Drugs* 3 is a program for filtering large compound libraries prior to *in silico* modeling studies. The tool can perform computational prediction of some ADME-tox properties (*Adsorption, Distribution, Metabolism, Excretion, and Toxicity*) and offers free online services for calculation of important molecular properties (LogP, polar surface area, number of hydrogen bond donors, and number of hydrogen bond acceptors), as well as prediction of the bioactivity score for the most important drug targets.

Table 2. Analyses of aggregation-prone amino acid residues in the Aβ₁₋₄₂ peptide sequence.

Amino acid sequence	Leu	Val	Phe	Ala	Ala	Glu	Asp	Val	Gly	Ser	Asn	Lys	Gly	Ala	Ile	Ile	Gly	Leu	Met	Val	Gly	Gly	Val	Val	Ile	Ala
1 ------------- 6	17	18	19	20	21	22	23	24	25	26	27	28	29	30	31	32	33	34	35	36	37	38	39	40	41	42
FoldAmyloid[1]								▓	▓	▓	▓	▓												▓	▓	
AGGRESCAN[2]								▓	▓	▓	▓	▓	▓										▓	▓	▓	▓
ProA[3]								▓	▓	▓	▓															

[1]FoldAmyloid [28], [2]AGGRESCAN [29], and [3]ProA [30] servers employ algorithms to predict amyloidogenic regions from protein amino acid sequence. The analyses are based on the amino acid physicochemical properties critical to protein aggregation. Color blocks indicate "common" amino acid residues those are prone to aggregation, as analyzed by [1,2,3]Different servers.
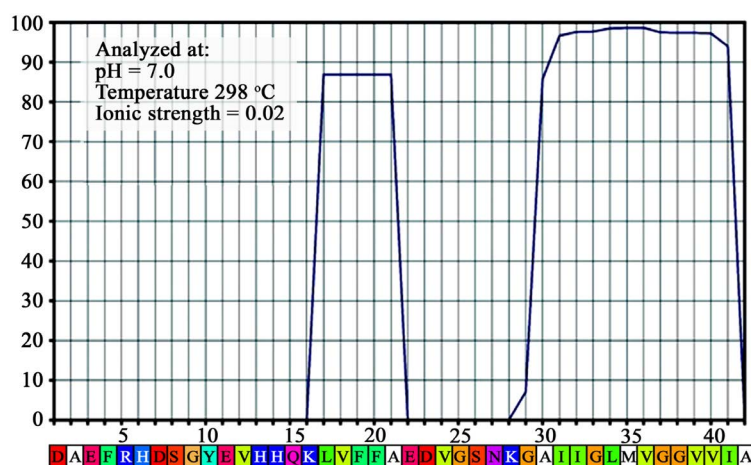
Figure 3. Beta-aggregation propensity analysis of Aβ₁₋₄₂. The red line indicates the region of the amino acid sequence (which is shown as single-alphabet strip) that induces beta aggregation.

we analyzed the protein-protein interface interaction sites for the A1B1 dimer. Because amyloid fibrillation starts with the interactions between at least two β strands, identifying these interaction sites is essential for understanding the nature of these sites, and whether DHA affects them, and the subsequent fibrillation. The Phe19 and Phe20 of the A1 monomer interacted with the Phe19 and Phe20 of the B1 monomer. The "Hot-point" server principally considers the solvent accessibility and total contact potential of the interface residues. The output file tabulates the interface residues with the highlighted hot spots and their features. The "hot-spot" with the highest potential was located in Leu34 on chain B1 of 2BEG. The KFC2 showed that the interaction sites were at Phe19 and Phe19 of A1 and B1. Other amino acids from either monomeric chain involved in the inter-surface interactions sites are highlighted in **Table 3**.

Pocketness is an important parameter that helps to determine the binding sites for ligands to their receptors. The 2BEG dimer or trimer showed ~5 or 6 pockets, whereas the 1Z0Q dimer displayed 4 pockets (**Figure 4**).

Docking performed by MVD provided the five best poses, and we obtained the corresponding MolDock score values and other thermodynamically calculated values. The 3D structures of the best scoring dockings are shown in **Figures 5(a)-(c)**. Steric interactions of ThT and DHA with Aβ₁₋₄₂ (the receptor) were also evaluated with MVD. Maps of the interactions of ThT with amino acid residues of the 2BEG dimer (A1B1) are shown in **Figure 5(a1)**. The docking of DHA to dimeric Aβ₁₋₄₂ (A1B1 of 2BEG and A1A2 of 1Z0Q) and their interaction maps are shown in **Figure 5(b)**, **Figure 5(b1)**, and **Figure 5(c)**, **Figure 5(c1)**, respectively. Using MVD, DHA had a MolDock score of −122.40 Kcal/mol and −140.40 Kcal/mol when docked onto the 2BEG and 1Z0Q dimers, respectively. The ThT reference molecule had a MolDock score of −130.37 Kcal/mol when docked onto the 2BEG dimer. Therefore, the binding of DHA to the 2BEG dimer was comparable with that of ThT, as demonstrated by similar binding energies (**Figure 5(b)**).

Amino acids involved in the docking of DHA to the Aβ₁₋₄₂ dimer (2BEG, A1B1) and Aβ₁₋₄₂ trimer (1Z0Q, A1A2) were visualized by contact maps of the interactions between atoms of DHA and the amyloid amino acid

Table 3. Analyses of momomer (A1)-monomer (B1) inter-surface interaction sites of Aβ_{1-42} dimer (A1-B1).

Amino acid sequence		Leu	Val	Phe	Ala	Ala	Glu	Asp	Val	Gly	Ser	Asn	Lys	Gly	Ala	Ile	Ile	Gly	Leu	Met	Val	Gly	Gly	Val	Val	Ile	Ala
1 ----------------- 6		17	18	19	20	21	22	23	24	25	26	27	28	29	30	31	32	33	34	35	36	37	38	39	40	41	42
PPISP[1]	A1			▓	▓															▓	▓	▓	▓		▓		
	B1		▒	▒	▒					▒			▒				▒	▒	▒		▒	▒	▒		▒		
Hotpoint[2]	A1																		▨								
	B1																										
KFC[3]	A1			▣		▣				▣									▨								
	B1												▣				▣		▣		▣		▣		▣		

[1]Cons-PPISP is a consensus neural network method for predicting protein-protein interaction sites. Given the structure of a protein, cons-PPISP will predict the residues that will likely form the binding site for another protein. The inputs to the neural network include position-specific sequence profiles and solvent accessibilities of each residue and its spatial neighbors. The neural network is trained on known structures of protein-protein complexes [38]. [2]Hotpoint: Hotpoint, which predicts hot spots in protein interfaces using an empirical model. The empirical model incorporates a few rules consisting of occlusion from solvent and total knowledge-based pair potentials of residues [39]. [3]KFC2 (Knowledge-based FADE and Contacts) server predicts binding "hot spots" within protein-protein interfaces by recognizing structural features indicative of important binding contacts. The server analyzes several chemical and physical features surrounding an interface residue and predicts the classification of the residue using a model trained on prior experimental data. Color blocks indicate "common" amino acid residues those acting at the inter-surface interaction sites, as the Aβ_{1-42} was analyzed by different servers.

(a) 2BEG dimer

(a1) Residue-based Pocket graph

(b) 2BEG trimer

(b1) Residue-based Pocket graph

(c) IZ0Q dimer

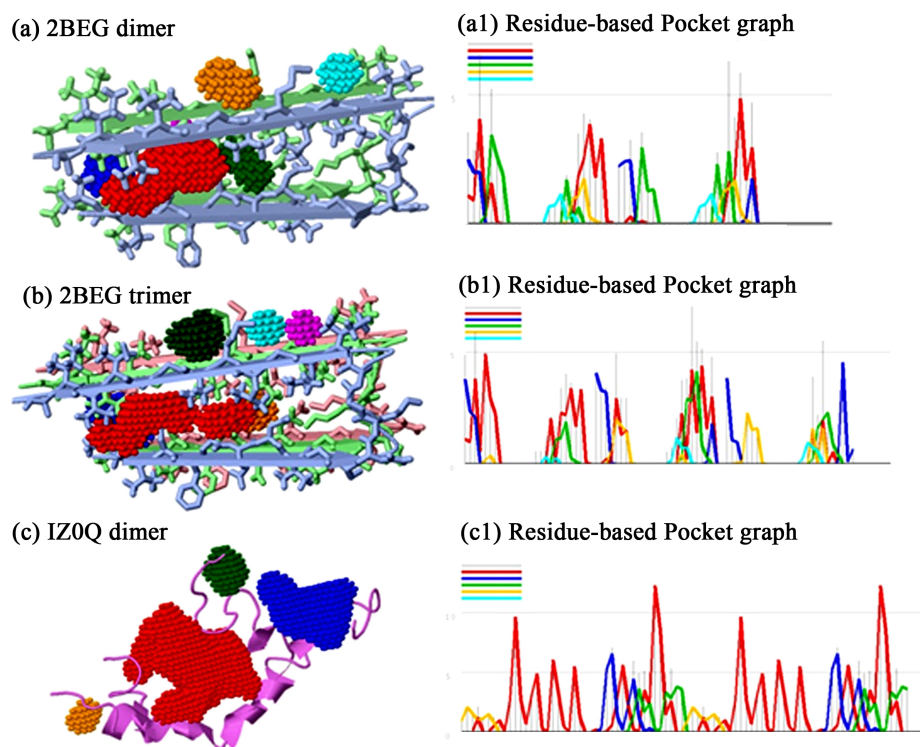(c1) Residue-based Pocket graph

Figure 4. Binding sites (pockets) analysis of Aβ_{1-42}. One of the simplest ways to predict ligand binding sites is to identify pocket-shaped regions on the protein surface. A binding sites or a pocket is defined as a space into which a small probe can enter, but a large probe cannot. A pocket intrinsically has two arbitrary properties, size and depth. The GHECOM analyzes these pockets using probe spheres. The radii of the probe spheres are assumed to correspond to the size and depth of the pockets. These values can be adjusted to individual putative ligand molecule. The binding sites or pockets of the dimer (A1B1) and trimer (A1B1C1) were determined by GHECOM, which detects grid-based pockets/binding sites on the surface/interior of the protein [36]. The presence of binding sites was visualized using the 3D molecular viewer Jmol [37]. The program also produces a graph of residue-based "pocketness" (right panel). (a1), (b1), (c1) number and position of amino acids (represented as lines on the primary sequences) involved in each of the pocket of (a), (b) and (c) of the left panel. For details please see Reference [36]. The individual color indicates the presence of distinct pockets.
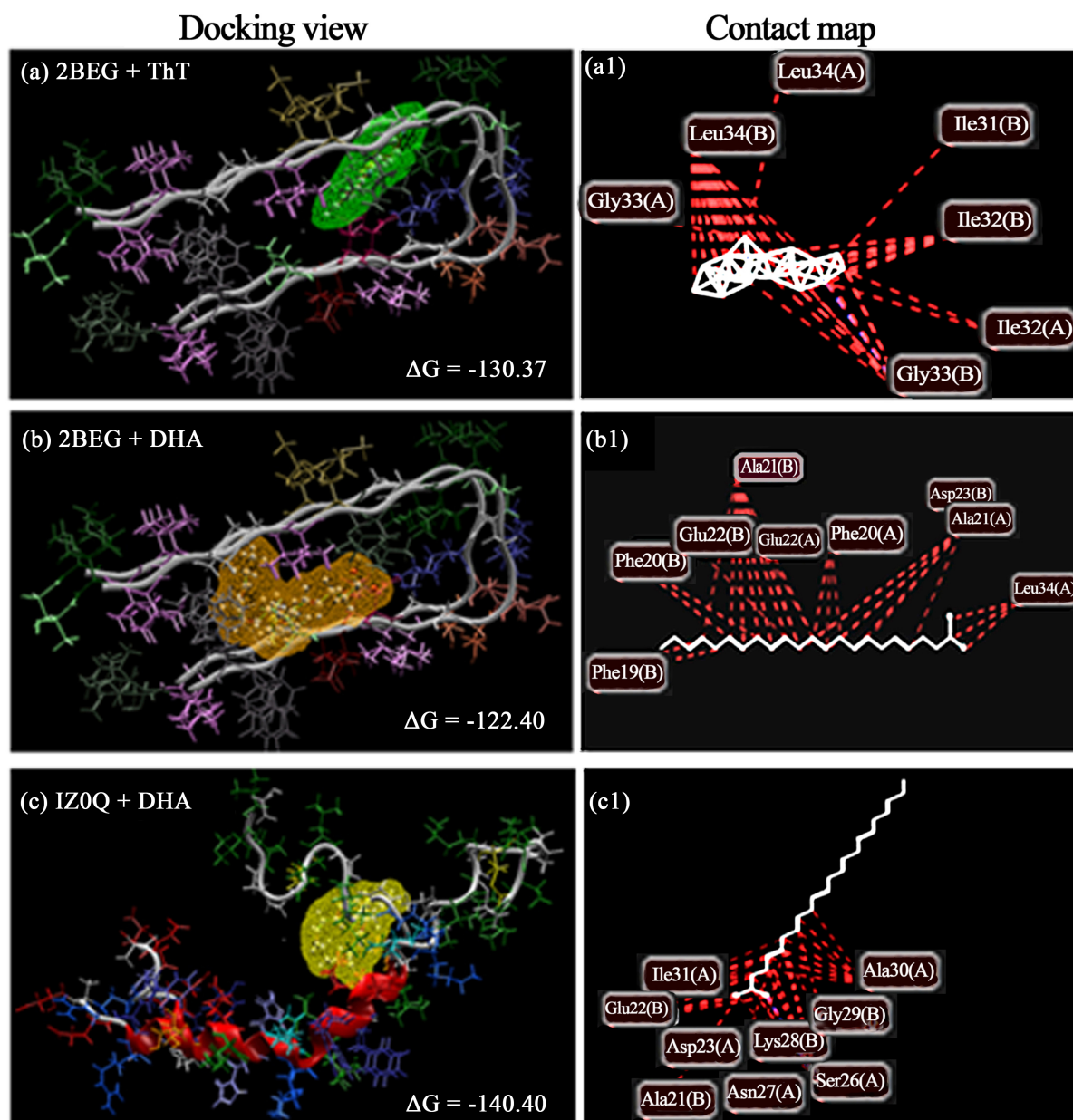
Docking view

(a) 2BEG + ThT

ΔG = -130.37

(b) 2BEG + DHA

ΔG = -122.40

(c) IZ0Q + DHA

ΔG = -140.40

Contact map

(a1)

Leu34(A)

Leu34(B)

Gly33(A)

Ile31(B)

Ile32(B)

Ile32(A)

Gly33(B)

(b1)

Ala21(B)

Glu22(B) Glu22(A) Phe20(A)

Phe20(B)

Asp23(B)

Ala21(A)

Leu34(A)

Phe19(B)

(c1)

Ile31(A)

Glu22(B)

Asp23(A) Lys28(B)

Ala21(B) Asn27(A)

Ala30(A)

Gly29(B)

Ser26(A)

Figure 5. The best-scored docking poses of ThT and DHA with the receptor (Aβ_{1-42}) by the MVD. (a) ThT docked onto the 2BEG A1B1 dimer. (b) DHA docked onto the 2BEG A1B1dimer. (c) DHA docked on the 1Z0Q A1A2 dimer. Interaction (binding) energies (ΔG) are also shown. Contact (binding) maps of the interactions between atoms of ThT/DHA and amino acid residues of the 2BEG/1Z0Q dimer are shown in the right panel (a1) (b1) and (c1). Contact maps were visualized by the "Ligand map" module of the MVD.

residues using MVD (**Figure 5(b1)** & **Figure 5(c1)**, and **Table 4**). The amino acid residues of the A1B1 dimer found to sterically interact with ThT were Ile32, Gly33, and Leu34 of A1 as well as Ile31, Ile32, Gly33, and Leu34 of B1.

We also performed molecular docking of ThT and DHA using PatchDock to confirm the ability of DHA to bind the 2BEG A1B1 dimer and the 2BEG A1B1C1 trimer (**Figure 6**). The algorithm used in PatchDock performs rigid docking, with surface variability/flexibility implicitly addressed through liberal intermolecular penetration. Geometric shape complementarity scores were similar for DHA and ThT when docked with the dimer (Score: ThT = 3742; DHA = 3732). However, there was higher shape complementarity when DHA was docked

onto the trimer (Score: ThT = 3632; DHA = 4326). Approximate complex interface areas (receptor-ligand) were also higher for DHA. ACEs for ThT and DHA were almost similar during docking onto the dimer; however, it was slightly higher for ThT when docked onto the trimer (**Table 5**). These data suggest that DHA and ThT have similar binding affinities.

Table 4. Patch docking of ThT and DHA with the 2BEG amyloid dimer (A1B1) and trimer (A1B1C1).

Docking (receptor vs. ligands)	Score	Area	ACE
A1B1 dimer vs. ThT	3742	445.40	−248.98
A1B1 dimer vs. DHA	3732	496.70	−241.07
A1B1C1 trimer vs. ThT	3632	4.33.6	−219.71
A1B1C1 trimer vs. DHA	4326	542.10	−198.30

Abbreviations: Score, geometric shape complementarity score; Area, approximate interface area of the complex (receptor-ligand); ACE, atomic contact energy; A1B1 dimer, generated by feeding the A1 and B1 model 1 of 2BEG to the Rosetta Server; A1B1C1 trimer, generated by feeding the A1, B1, and C1 coordinate model 1 of 2BEG to the Rosetta Server; ThT, thioflavin T; DHA, docosahexaenoic acid.

Table 5. Summary of dockink of DHA and ThT on to NMR structures of $A\beta_{1-42}$ dimer structures (A1B1 of 2BEG and A1A2 of 1Z0Q).

Amino acid sequence			Leu	Val	Phe	Ala	Ala	Glu	Asp	Val	Gly	Ser	Asn	Lys	Gly	Ala	Ile	Ile	Gly	Leu	Met	Val	Gly	Gly	Val	Val	Ile	Ala
1 ----------------------- 6			17	18	19	20	21	22	23	24	25	26	27	28	29	30	31	32	33	34	35	36	37	38	39	40	41	42
DHA	2BEG	A1				▮ red	▮ red	▮ red												▮ red									
		B1			▮ red	▮ red	▮ red	▮ red																					
	1Z0Q	A1							▮ yellow			▮ yellow	▮ yellow			▮ yellow													
		B1				▮ yellow	▮ yellow							▮ yellow	▮ yellow		▮ yellow												
ThT	2BEG	A1																▮ blue	▮ blue	▮ blue									
		B1															▮ blue	▮ blue	▮ blue	▮ blue									

When DHA and ThT were docked onto 2BEG dimer, they shared a common binding site at Ile31of A1 peptide. Both the 2BEG and 1Z0Q pdb had common binding sites at Ala21 of A1 and Glu21 of B1 peptide. Color blocks at a given position (of the sequence) indicate common binding sites for the ligand.

Figure 6. The best scoring results of the Patch Dock for ThT (a)-(c) and DHA (b)-(d) with the A1B1 dimer (a) (b) and the A1B1C1 trimer (c) (d). Ligands (ThT and DHA) are represented by green sticks, and the receptors (dimer and trimer) are shown as β-sheet ribbons with the amino acid side chains presented as sticks.

The ligand-docked receptor obtained from PatchDock was visualized using PyMOL as shown in **Figure 6**. ThT bound with the interior regions of both the dimer and trimer (**Figure 6(a)** & **Figure 6(c)**), whereas DHA was found to wrap around the β-sheet of the dimer (**Figure 6(b)** & **Figure 6(d)**).

4. Discussion

Alzheimer's disease (AD) is one of the most common chronic dementia-related diseases worldwide, and the number of AD patients is increasing every year. Currently, only two medications (cholinesterase inhibitors and an NMDA receptor antagonist) are approved by the United States Food and Drug Administration [44] to treat the cognitive symptoms (memory loss and confusion) of AD. However, these medications cannot cure AD or arrest its progression. Vitamins or other supplements, such as omega-3 fatty acids [45], and various herbal mixtures are also widely promoted as preparations that may support cognitive health or prevent or delay AD. The NIH panel concluded that there is somewhat stronger data—but not definitive evidence—that omega-3 fatty acids in fish oil may help prevent cognitive decline. The basis of such conclusion might relate to the fact that the concentration of omega-3 polyunsaturated docosahexaenoic acid (DHA, C22:6, n-3) is significantly reduced in the brains of AD patients [21] [22]. We also reported on the beneficial effects of dietary omega-3 polyunsaturated fatty acid supplementation on age-related cognitive decline in elderly Japanese patients with very mild dementia [46]. Therefore, DHA supplementation may decelerate the cognitive symptoms of AD.

We previously showed that chronic administration of DHA significantly decreased the amyloid burden in the brains of AD model rats [14]. DHA also inhibited the *in vitro* amyloid fibrillations of A$\beta_{1\text{-}40}$ [16], A$\beta_{1\text{-}42}$ [10], and A$\beta_{25\text{-}35}$ [18], indicating that neurotoxicity convened by these amyloid species would be inhibited by the DHA. Moreover, we found that A$\beta_{1\text{-}42}$-induced toxicity of SH-S5Y5 cells was reduced by DHA [10], andour previous transmission electron microscopy, laser-scanning fluorescence microscopy, and thioflavin T fluorospectroscopy studies clearly indicated that DHA resists fibrillogenesis by some unknown mechanism [10] [16] [18]. Despite strong evidences that soluble forms of Aβ are toxic at synapses, the exact forms of the toxic species remain to be determined. There is evidence for toxicity of both low molecular weight dimers and trimers of Aβ [47]-[50]. Using Western blot analysis and/or polyacrylamide gel electrophoresis, we have also shown that DHA inhibits the fibrillation of dimeric/trimeric and oligomeric Aβs [10]; thus, it ultimately decreases the elongation process of amyloid fibrillation leading to matured fibers. Finally, the anti-Aβ fibrillation effect of DHA was further supported by the reductions of Aβ-induced apoptosis and neurodegeneration [10] in DHA-treated cell culture. These *in vivo/in vitro* experimental data strongly suggest that DHA prevents amyloid peptides from forming toxic species that ultimately deteriorate memory and other behavioral aspects in AD patients.

These findings also demonstrate that Aβ peptides are important drug targets, and designing drugs that disrupt the formation of Aβ-Aβ inter-surface interaction sites is particularly important for preventing Aβ fiber formation. Therefore, we performed the present *in silico* study to support the experimentally proven ameliorative effects of DHA on the Aβ-fibrillation. Accordingly, we modeled the 3D structure of DHA and used docking simulation to determine whether DHA binds to Aβ peptides and to predict the affinity between the ligand (DHA) and the receptor (Aβ). During docking simulations with both MVD and PatchDock, we used ThT as a positive control to verify whether docking would yield ligand geometry similar to that of DHA when binding to Aβ peptides.

Using MVD, DHA had a MolDock score of −122.4 Kcal/mol with 2BEG, and −140.40 Kcal/mol with 1Z0Q, whereas ThT had a MolDock score of −130.37 Kcal/mol. These results suggest considerable binding of DHA with the dimeric A$\beta_{1\text{-}42}$ molecules. This might explain the reduced amyloid burden observed in the brains of DHA-administered AD model rats [16] and concurrent inhibition of *in vitro* fibril formation [10]. Monomer-monomer inter-surface interaction site analyses revealed that Phe19 (A1) and Phe19 (B1) were the common amino acid residues, which acted as monomer-monomer inter-surface interaction sites (**Table 3**). Other amino acid residues, including Phe20 (A1), Phe20 (B1), Ala21 (A1), Asp23 (A1), Gly25 (A1), Lys28 (B1), Ile32 (B1), Gly33 (A1), Leu34 (B1), Met (A1), Val36 (A1), Val36 (B1), Gly37 (A1), Gly37 (B1), Gly38 (A1), Val39 (B1), Val 40 (A1), and Ile41 (B1) also acted as inter-surface interaction sites (**Table 3**). These inter-surface interaction sites might have been targeted by the DHA, as indicated by the interactions of DHA with these amino acid regions, particularly, those of Phe19, Ala21, Asp23, and Leu34. Notably, DHA also interacted with Ala21, Glu22, Asp23, and Ser26-Ile31 of 1Z0Q, which is in an α-helix random coil conformation rather than the β-sheet conformation that is the prerequisite for the propagation of fibrillation. As shown in **Table 2**, the amino acid residues 24 - 29 and 39 - 42 are the most aggregation-sensitive regions of A$\beta_{1\text{-}42}$. All these results suggest that DHA

interacts with these aggregation-prone monomer-monomer inter-surface interaction sites. Moreover, ThT docked with 2BEG in a similar manner to DHA and bound to Ile31, Ile32, Gly33, and Leu34.

In the PatchDock system, the docking of DHA and ThT were similar, as indicated by the almost similar docking score. However, when they were docked by PatchDock onto the Aβ_{1-42} trimer, DHA displayed a greater binding affinity (score) than ThT. When the PatchDock receptor-ligand was visualized with PyMOL (**Figure 6**), an interesting feature was obtained: DHA spirally wrapped the dimer, whereas ThT bound to the interior of the dimer. Notably, DHA and ThT both bound to the predicted binding pockets (**Figure 4**). The binding interaction between the ligand molecule (DHA) and receptor (Aβ_{1-42}) has a significant role in determining the anti-amyloid activity. Therefore, the binding potential of DHA in this computational study supports the results of our previous *in vivo* and *in vitro* biological studies showing that DHA decreases *in vitro* amyloid fibrillation and amyloid brain burden in a rat AD model, with concurrent amelioration of Aβ-induced memory loss [10] [14] [16] [18]. AD drug discovery has been a very lengthy and costly process, and the prevention of AD remains a burning issue worldwide. Polyunsaturated fatty acids, including DHA, have been continually investigated over the last several years as potential drug candidates with minimal side effects in experimental animal models of AD and/or AD human patients. Using a targeted and more specific approach for future high-throughput screens, such as those based on the results of similar *in silico* experiments performed here, we may be able to more rapidly identify novel AD drugs.

5. Conclusion

Computational drug design is a promising method for discovering many more drugs in the coming years. Here we demonstrated that molecular docking of DHA is consistent with its anti-amyloid effects, in particular, on *in vitro* fibrillation and *in vivo* Aβ-induced memory impairments of AD model rats. Our study further reaffirms that DHA is important for the structure and biological function of Aβs. We also showed that scoring the docking values gives the best prediction for ligand interactions with proteins. Finally, our *in silico* results provide compelling evidence for the utility of DHA as a preventive medication for neurodegenerative diseases such as Aβ_{1-42}-induced AD. Further studies on DHA-like molecules hold promise for the development of anti-amyloid drugs.

Acknowledgements

Conflict of Interest

The authors declare no-conflict of interest.

References

[1] Rajan, K.B., Wilson, R.S., Weuve, J., Barnes, L.L. and Evans, D.A. (2015) Cognitive Impairment 18 Years before Clinical Diagnosis of Alzheimer Disease Dementia. *Neurology*.

[2] Sindi, S., Mangialasche, F. and Kivipelto, M. (2015) Advances in the Prevention of Alzheimer's Disease. *F1000Prime Reports*, **7**, 50. http://dx.doi.org/10.12703/P7-50

[3] Bacanu, S.A., Devlin, B., Chowdari, K.V., DeKosky, S.T., Nimgaonkar, V.L. and Sweet, R.A. (2005) Heritability of Psychosis in Alzheimer Disease. *American Journal of Geriatric Psychiatry*, **13**, 624-627. http://dx.doi.org/10.1097/00019442-200507000-00011

[4] Selkoe, D.J. (1991) The Molecular Pathology of Alzheimer's Disease. *Neuron*, **6**, 487-498. http://dx.doi.org/10.1016/0896-6273(91)90052-2

[5] Citron, M. (2010) Alzheimer's Disease: Strategies for Disease Modification. *Nature Reviews Drug Discovery*, **9**, 387-398. http://dx.doi.org/10.1038/nrd2896

[6] De Strooper, B., Vassar, R. and Golde, T. (2010) The Secretases: Enzymes with Therapeutic Potential in Alzheimer Disease. *Nature Reviews Neuroscience*, **6**, 99-107. http://dx.doi.org/10.1038/nrneurol.2009.218

[7] Golde, T.E., Schneider, L.S. and Koo, E.H. (2011) Anti-Aβ Therapeutics in Alzheimer's Disease: The Need for Apa-

radigm Shift. *Neuron*, **69**, 203-213. http://dx.doi.org/10.1016/j.neuron.2011.01.002

[8]   Huang, Y. and Lennart Mucke, L. (2012) Alzheimer Mechanisms and Therapeutic Strategies. *Cell*, **148**, 1204-1222. http://dx.doi.org/10.1016/j.cell.2012.02.040

[9]   Palop, J.J. and Mucke, L. (2010) Amyloid-Beta-Induced Neuronal Dysfunction in Alzheimer's Disease: From Synapses toward Neural Networks. *Nature Neuroscience*, **13**, 812-818. http://dx.doi.org/10.1038/nn.2583

[10] Hossain, S., Hashimoto, M., Katakura, M., Miwa, K., Shimada, T. and Shido, O. (2009) Mechanism of Docosahexaenoicacid-Induced Inhibition of *in Vitro* Aβ_{1-42} Fibrillation and Aβ_{1-42}-Induced Toxicity in SH-S5Y5 Cells. *Journal of Neurochemistry*, **111**, 568-579. http://dx.doi.org/10.1111/j.1471-4159.2009.06336.x

[11] Goedert, M. and Spillantini, M.G. (2006) A Century of Alzheimer's Disease. *Science*, **314**, 777-781. http://dx.doi.org/10.1126/science.1132814

[12] Song, Y., Chen, X., Wang L.Y., Gao, W. and Zhu, M.J. (2013) Rho Kinase Inhibitor Fasudil Protects Against β-Amyloid-Induced Hippocampal Neurodegeneration in Rats. *CNS Neuroscience & Therapeutics*, **19**, 603-610. http://dx.doi.org/10.1111/cns.12116

[13] Mamun, A.A., Hashimoto, M., Katakura, M., Matsuzaki, K., Hossain, S., Arai, H. and Shido, O. (2014) Neuroprotective Effect of Madecassoside Evaluated Using Amyloid B1-42-Mediated *in Vitro* and *in Vivo* Alzheimer's Disease Models. *International Journal of Indigenous Medicinal Plants*, **47**, 1669-1682.

[14] Hashimoto, M., Hossain, S., Shimada, T., Sugioka, K., Yamasaki, H., Fujii, Y., Ishibashi, Y., Oka, J. and Shido, O. (2002) Docosahexaenoic Acid Provides Protection from Impairment of Learning Ability in Alzheimer's Disease Model Rats. *Journal of Neurochemistry*, **81**, 1084-1091. http://dx.doi.org/10.1046/j.1471-4159.2002.00905.x

[15] Hashimoto, M., Hossain, S. and Shido, O. (2005) Docosahexaenoic Acid-Induced Amelioration on Impairment of Memory Learning in Amyloid Beta-Infused Rats Relates to the Decreases of Amyloid Beta and Cholesterol Levels in Detergent-Insoluble Membrane Fractions. *Biochimica et Biophysica Acta*, **1738**, 91-98. http://dx.doi.org/10.1016/j.bbalip.2005.11.011

[16] Hashimoto, M., Shahdat, H.M., Yamashita, S., Katakura, M., Tanabe, Y., Fujiwara ,H., Gamoh, S., Miyazawa, T., Arai H., Shimada, T. and Shido, O. (2008) Docosahexaenoic Acid Disrupts *in Vitro* Amyloid Beta(1-40)Fibrillation and Concomitantly Inhibits Amyloid Levels in Cerebral Cortex of Alzheimer's Disease Modelrats. *Journal of Neurochemistry*, **107**, 1634-1646. http://dx.doi.org/10.1111/j.1471-4159.2008.05731.x

[17] Kubo, T., Nishimura, S., Kumagae, Y. and Kaneko, I. (2002) *In Vivo* Conversion of Racemized β-Amyloid ([D-Ser^{26}] Aβ_{1-40}) to Truncated and Toxic Fragments ([D-Ser^{26}]A$\beta_{25-35/40}$) and Fragment Presencein the Brains of Alzheimer's Patients. *Journal of Neuroscience Research*, **70**, 474-483. http://dx.doi.org/10.1002/jnr.10391

[18] Hashimoto, M., Shahdat, H.M., Katakura, M., Tanabe, Y., Gamoh, S., Miwa, K., Shimada, T. and Shido, O. (2009) Effects of Docosahexaenoic Acid on *in Vitro* Amyloid Beta Peptide 25-35 Fibrillation. *Biochimica et Biophysica Acta*, **1791**, 289-296. http://dx.doi.org/10.1016/j.bbalip.2009.01.012

[19] Soderberg, M., Edlund, C., Kristensson, K. and Dallner, G. (1991) Fatty Acid Composition of Brain Phospholipidsin Aging and in Alzheimer's Disease. *Lipids*, **26**, 421-425. http://dx.doi.org/10.1007/BF02536067

[20] Prasad, M.R., Lovell, M.A., Yatin, M., Dhillon, H. and Markesbery, W.R. (1998) Regional Membrane Phospholipidalterations in Alzheimer's Disease. *Neurochemical Research*, **23**, 81-89. http://dx.doi.org/10.1023/A:1022457605436

[21] Morris, M.C., Evans, D.A., Bienias, J.L., Tangney, C.C., Bennett, D.A., Wilson, R.S., Aggarwal, N. and Schneider, J. (2003) Consumption of Fish and n-3 Fatty Acids and Risk of Incident Alzheimer Disease. *Archives of Neurology*, **l60**, 940-946. http://dx.doi.org/10.1001/archneur.60.7.940

[22] Huang, T.L., Zandi, P.P., Tucker, K.L., Fitzpatrick, A.L., Kuller, L.H., Fried, L.P., Burke, G.L. and Carlson, M.C. (2005) Benefits of Fatty Fish on Dementia Risk Are Stronger for Those without *APOE* Epsilon4. *Neurology*, **65**, 1409-1414. http://dx.doi.org/10.1212/01.wnl.0000183148.34197.2e

[23] Mamun, A.A., Hashimoto, M., Hossain, S., Katakura, M., Matsuzaki, K., Arai, H. and Shido, O. (2015) Confirmation of the Experimentally-Proven Therapeutic Utility of Madecassoside in an Aβ_{1-42} InfusionRat Model of Alzheimer's Disease by *in Silico* Analyses. *Advances in Alzheimer's Disease*, **4**, 37-44. http://dx.doi.org/10.4236/aad.2015.42005

[24] Schüttelkopf, A.W. and van Aalten, D.M.F. (2004) PRODRG—A Tool for High-Throughput Crystallography of Protein-Ligand Complexes. *Acta Crystallographica*, **D60**, 1355-1363. http://dx.doi.org/10.1107/S0907444904011679

[25] Lipinski, C.A., Lombardo, F., Dominy, B.W. and Feeney, P.J. (2001) Experimental and Computational Approaches to Estimate Solubility and Permeability in Drug Discovery and Development Settings. *Advanced Drug Delivery Reviews*, **46**, 3-26. http://dx.doi.org/10.1016/S0169-409X(00)00129-0

[26] Ertl, P., Rohde, B. and Selzer, P. (2000) Fast Calculation of Molecular Polar Surface Area as a Sum of Fragment-Based Contributions and Its Application to the Prediction of Drug Transport Properties. *Journal of Medicinal Chemistry*, **43**, 3714-3717. http://dx.doi.org/10.1021/jm000942e

[27] Daylight Chemical Information Systems Inc. (2007) SMARTS—A Language for Describing Molecular Patterns. Aliso Viejo.

[28] Garbuzynskiy, S.O., Lobanov, M.Y. and Galzitskaya, O.V. (2010) Fold Amyloid: A Method of Prediction Ofamyloidogenic Regions from Protein Sequence. *Bioinformatics* (*Oxford*, *England*), **26**, 326-332. http://dx.doi.org/10.1093/bioinformatics/btp691

[29] Conchillo-Sole, O., de Groot, N.S., Aviles, F.X., Vendrell, J., Daura , X. and Ventura, S. (2007) AGGRESCAN: Aserver for the Prediction and Evaluation of "Hot Spots" of Aggregation in Polypeptides. *BMC Bioinformatics*, **8**, 65. http://dx.doi.org/10.1186/1471-2105-8-65

[30] Fang, Y., Gao, S., Ta, D., Middaugh, C.R. and Fang, J. (2013) Identification of Properties Important to Protein Aggregation Using Feature Selection. *BMC Bioinformatics*, **14**, 314. http://dx.doi.org/10.1186/1471-2105-14-314

[31] Rousseau, F., Schymkowitz, J. and Serrano, L. (2006) Protein Aggregation and Amyloidosis: Confusion of the Kinds? *Current Opinion in Structural Biology*, **16**, 118-126. http://dx.doi.org/10.1016/j.sbi.2006.01.011

[32] Fernandez-Escamilla A.M., Rousseau, F., Schymkowitz, J. and Serrano, L. (2004) Prediction of Sequence-Dependent and Mutational Effects on the Aggregation of Peptides and Proteins. *Nature Biotechnology*, **22**, 1302-1306. http://dx.doi.org/10.1038/nbt1012

[33] Linding, R., Schymkowitz, J., Rousseau, F., Diella, F. and Serrano, L. (2004) A Comparative Study of the Relationship between Protein Structure and Beta-Aggregation in Globular and Intrinsically Disordered Proteins. *Journal of Molecular Biology*, **342**, 345-353. http://dx.doi.org/10.1016/j.jmb.2004.06.088

[34] Lyskov, S. and Gray, J.J. (2008) The RosettaDock Server for Local Protein-Protein Docking. *Nucleic Acids Research*, **36**, W233-W238. http://dx.doi.org/10.1093/nar/gkn216

[35] Hossain, S., Hashimoto, M., Katakura, M., Mamun, A.A. and Shido, O. (2015) Medicinal Value of Asiaticoside for Alzheimer's Disease as Assessed Using Single-Molecule-Detection Fluorescence Correlation Spectroscopy, Laser-Scanning Microscopy, Transmission Electron Microscopy, and *in Silico* Docking. *BMC Complementary and Alternative Medicine*, **15**, 118. http://dx.doi.org/10.1186/s12906-015-0620-9

[36] Kawabata, T. (2010) Detection of Multi-Scale Pockets on Protein Surfaces Using Mathematical Morphology. *Proteins*, **78**, 1195-1221. http://dx.doi.org/10.1002/prot.22639

[37] Jmol: An Open-Source Java Viewer for Chemical Structures in 3D. http://www.jmol.org/

[38] Chenm, H.-L. and Zhou, H.-X. (2005) Prediction of Interface Residues in Protein-Protein Complexes by a Consensus Neural Network Method: Test against NMR Data. *Proteins*, **61**, 21-35. http://dx.doi.org/10.1002/prot.20514

[39] Tuncbag, N., Gursoy, A. and Keskin, O. (2009) Identification of Computational Hotspots in Protein Interfaces: Combining Solvent Accessibility and Inter-Residue Potentials Improves the Accuracy. *Bioinformatics*, **25**, 1513-1520. http://dx.doi.org/10.1093/bioinformatics/btp240

[40] Zhu, X. and Mitchell, J.C. (2011) KFC2: A Knowledge-Based Hot Spot Prediction Method Based on Interface Solvation, Atomic Density and Plasticity Features. *Proteins*, **79**, 2671-2683. http://dx.doi.org/10.1002/prot.23094

[41] Thomsen, R. and Christensen M.H. (2006) MolDock: A New Technique for High-Accuracy Molecular Docking. *Journal of Medicinal Chemistry*, **49**, 3315-3321. http://dx.doi.org/10.1021/jm051197e

[42] Duhovny, D., Nussinov, R., Wolfson, H.J., *et al*. (2002) Efficient Unbound Docking of Rigid Molecules. *Proceedings of the* 2*nd Workshop on Algorithms in Bioinformatics* (*WABI*), Vol. 2452, Rome, 17-21 September 2002, 185-200. http://dx.doi.org/10.1007/3-540-45784-4_14

[43] The PyMOL (1.7.4.4 Edu) Molecular Graphics System, Version 1.8 Schrödinger, LLC.

[44] http://www.alz.org/research/science/alzheimers_disease_treatments.asp#approved

[45] http://www.alz.org/professionals_and_researchers_alternative_treatments_.asp#omega

[46] Hashimoto, M., Yamashita, K. and Kato, S. (2012) Beneficial Effects of Dietary Omega-3 Polyunsaturated Fatty Acid Supplementation on Age-Related Cognitive Decline in Elder Japanese with Very Mild Dementia: A 2-Year Randomized, Double-Blind, Placebo-Controlled Trial. *The Journal of Aging Research & Clinical Practice*, **1**, 193-201.

[47] Jin, M., Shepardson, N., Yang, T., Chen, G., Walsh, D. and Selkoe, D. (2011) Soluble Amyloid Beta-Protein Dimers Isolated from Alzheimer Cortex Directly Induce Tau Hyperphosphorylation and Neuritic Degeneration. *Proceedings of the National Academy of Sciences of the United States of America*, **108**, 5819-5824. http://dx.doi.org/10.1073/pnas.1017033108

[48] Masters, C. and Selkoe, D. (2012) Biochemistry of Amyloid *β*-Protein and Amyloid Deposits in Alzheimer Disease. *Cold Spring Harbor Perspectives in Medicine*, **2**, a006262. http://dx.doi.org/10.1101/cshperspect.a006262

[49] Mc Donald, J., Savva, G., Brayne, C., Welzel, A., Forster, G., Shankar, G., Selkoe, D., Ince, P. and Walsh, D. (2010) Medical Research Council Cognitive F and Ageing S. The Presence of Sodium Dodecyl Sulphatestable Abeta Dimers

Is Strongly Associated with Alzheimer-Type Dementia. *Brain*, **133**, 1328-1341.
http://dx.doi.org/10.1093/brain/awq065

[50] Shankar, G.M., Li, S., Mehta, T.H., Garcia-Munoz, A., Shepardson, N.E., Smith, I., Brett, F.M., Farrell, M.A., Rowan, M.J., Lemere, C.A., *et al*. (2008) Amyloid-Beta Protein Dimers Isolated Directly from Alzheimer's Brains Impair Synaptic Plasticity and Memory. *Nature Medicine*, **14**, 837-842. http://dx.doi.org/10.1038/nm1782

Abbreviations Used

AD: Alzheimer's Disease;
Aβ: Amyloid Beta Peptide;
RCSB: Research Collaboratory for Structural Bioinformatics;
PBD: Protein Data Bank;
MVD: Molegro Virtual Docker;
ThT: Thioflavin T;
DHA: Docosahexaenoic Acid